Journal of Solid Mechanics Vol. 8, No. 2 (2016) pp. 334-347

Semi-Analytical Solution for Free Vibration Analysis of Thick Laminated Curved Panels with Power-Law Distribution FG Layers and Finite Length Via Two-Dimensional GDQ Method

V. Tahouneh[1] , M.H. Naei [2, *]

[1] *Young Researchers and Elite Club, Islamshahr Branch, Islamic Azad University, Islamshahr, Iran*
[2] *School of Mechanical Engineering, College of Engineering, University of Tehran, Tehran, Iran*

Received 25 February 2016; accepted 20 April 2016

ABSTRACT

This paper deals with free vibration analysis of thick Laminated curved panels with finite length, based on the three-dimensional elasticity theory. Because of using two-dimensional generalized differential quadrature method, the present approach makes possible vibration analysis of cylindrical panels with two opposite axial edges simply supported and arbitrary boundary conditions including Free, Simply supported and Clamped at the curved edges. The material properties vary continuously through the layers thickness according to a three-parameter power-low distribution. It is assumed that the inner surfaces of the FG sheets are metal rich while the outer surfaces of the layers can be metal rich, ceramic rich or made of a mixture of two constituents. The benefit of using the considered power-law distribution is to illustrate and present useful results arising from symmetric and asymmetric profiles. The effects of geometrical and material parameters together with the boundary conditions on the frequency parameters of the laminated FG panels are investigated. The obtained results show that the outer FGM Layers have significant effects on the vibration behavior of cylindrical panels. This study serves as a benchmark for assessing the validity of numerical methods or two-dimensional theories used to analysis of laminated curved panels.

Keywords : Semi-analytical solution; FG laminated structures; Finite length curved panels; Vibration analysis; Three-parameter power-low distribution.

1 INTRODUCTION

FUNCTIONALLY graded cylindrical panels, as important structural components, have widely been used in different branches of engineering such as mechanical, energy and aerospace engineering. However, in comparison with the isotropic and conventional laminated cylindrical panels, the literature on the free vibration analysis of FG cylindrical panels is relatively scarce. In addition, in the most of the existing researches in this regards, single layer FG cylindrical panels have been analyzed. In the following, some of these research works are briefly reviewed. Due to the mismatch of stiffness properties between the face sheets and the core, sandwich plates and panels are susceptible to face sheet/core debonding, which is a major problem in sandwich construction, especially under impact loading [1]. Various material profiles through the functionally graded plate and panel

*Corresponding author.
E-mail address: mhnaei@ut.ac.ir (M.H. Naei).

thickness can be illustrated by using three-parameter power-low distribution. In fact, by using this power-low distribution, it is possible to study the influence of the different kinds of material profiles. Recently, Viola and Tornabene [2] used three-parameter power-low distribution to study the dynamic behavior of functionally graded parabolic panels of revolution. Though there are research works reported on general sandwich structures, very little work has been done to consider the vibration behavior of FGM sandwich structures [3,4]. Li et al. [5] studied free vibrations of FGSW rectangular plates with simply supported and clamped edges. Zenkour [6,7] presented a two-dimensional solution to study the bending, buckling and free vibration of simply supported FG ceramic-metal sandwich plates. Kamarian et al. [8] studied free vibration of FGSW rectangular plates with simply supported edges and rested on elastic foundations using differential quadratic method. The natural frequencies of FGM circular cylindrical shells are investigated [9], which was later extended to cylindrical shells under various end supporting conditions [10]. Patel et al. [11] carried out the vibration analysis of functionally graded shell using a higher-order theory. Pradyumna et al. [12] studied the free vibrations analysis of functionally graded curved panels by using a higher-order finite element formulation. Free vibration and dynamic instability of FGM cylindrical panels under combined static and periodic axial forces were studied by using a proposed semi-analytical approach [13]. Elastic response analysis of simply supported FGM cylindrical shell under low-velocity impact was presented by Gang et al. [14]. Vibrations and wave propagation velocity in a functionally graded hollow cylinder were studied by Shakeri et al. [15]. They assumed the shell to be in plane strain condition and subjected to an axisymmetric dynamic loading. The free vibration of simply supported, fluid-filled cylindrically orthotropic functionally graded cylindrical shells with arbitrary thickness was investigated by Chen et al. [16]. Recently, Tornabene [17] used four-parameter power-law distribution to study the dynamic behavior of moderately thick functionally graded conical and cylindrical shells and annular plates. In his study, the two-constituent functionally graded isotropic shell was consisted of ceramic and metal, and the generalized differential quadrature method was used to discretize the governing equation. Static and free vibration analyses of continuously graded fiber-reinforced cylindrical shells using generalized power-law distribution are presented by Sobhani Aragh and Yas [18]. Also, these authors [19] investigated three-dimensional free vibration of functionally graded fiber orientation and volume fraction of cylindrical panels. Paliwal et al. [20,21] have investigated the free vibration of whole buried cylindrical shells with simply supported ends in contact with Winkler and Pasternak foundations using direct solution to the governing classical shell theory equations of motion. Yang et al. [22] have investigated the behavior of whole buried pipelines subjected to sinusoidal seismic waves by the finite element method. Cai et al. [23] have investigated free vibration of a cylindrical panel supported on Kerr foundation. Kerr model can be reduced to either a Pasternak model or a Winkler one by selecting certain values of foundation parameters. Gunawan et al. [24] examined the free vibrations of cylindrical shells partially buried in elastic foundations based on the finite element method. The shells are discretized into cylindrical finite elements, and the distribution of the foundation in the circumferential direction is defined by the expansion of Fourier series. Farid et al. [25] have studied three-dimensional temperature-dependent free vibration analysis of functionally graded material curved panels resting on two-parameter elastic foundation subjected in thermal environment. The curved panels was made of isotropic material, and in order to discretize the governing equations, the differential quadrature method in the thickness direction and the trigonometric functions in longitudinal and tangential directions in conjunction of the three-dimensional form of the Hamilton's principle have been used. Free vibration and stability of functionally graded shallow shells according to a 2-D higher order deformation theory were investigated by Matsunaga [26]. Civalek [27] has investigated the nonlinear dynamic response of doubly curved shallow shells resting on Winkler–Pasternak elastic foundation using the harmonic differential quadrature (HDQ) and finite differences (FD) methods.

To the authors' best knowledge, Studies about free vibration of thick FGSW structures are very limited in numbers. Furthermore, this paper is motivated by the lack of studies in the technical literature concerning to the effect of the parameters of power-law distributions on the vibration behavior of functionally graded laminated curved panels. Frequency parameters are obtained by using numerical technique termed the generalized differential quadrature method (GDQM), which leads to a generalized eigenvalue problem. The differential quadrature method (DQM) is found to be a simple and efficient numerical technique for vibration analysis of structures [28-33].

2 FUNCTIONALLY GRADED SANDWICH PROPERTIES

Consider an FGSW curved panel as shown in Fig. 1. A cylindrical coordinate system (r, ϑ, z) is used to label the material point of the panel. The panel has continuous grading of fiber reinforcement through radial direction. h, h_c

and h_s are the thickness of panel, core and face sheets, respectively. In the present work, the fiber volume fraction of laminated curved panel is assumed as follows:

$$V_C = \begin{cases} [1-(\dfrac{(r-R)+0.5h}{h_S})+b(1-\dfrac{(r-R)+0.5h}{h_S})^c]^p & -0.5h \le r-R \le -0.5h+h_S \\ 0 & -0.5h+h_S \le r-R \le 0.5h-h_S \\ [1-(\dfrac{-(r-R)+0.5h}{h_S})+b(1-\dfrac{-(r-R)+0.5h}{h_S})^c]^p & 0.5h-h_S \le r-R \le 0.5h \end{cases} \quad (1)$$

where the power-law index p $(0 \le p \le \infty)$ and the parameters b and c dictate the fiber variation profile through the radial direction of the panel. According to the above-mentioned relation the core of sandwich panel and the inner surfaces of the FG sheets are metal rich. The outer surfaces of the sheets can be metal rich, ceramic rich or made of a mixture of two constituents. The through-thickness variations of the fiber volume fraction of sandwich panel are shown in Figs. 2, 3, 4 and 5.

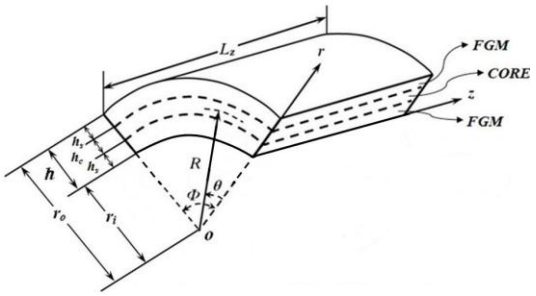

Fig.1
The sketch of a thick laminated curved panel with three-parameter FG outer layers and setup of the coordinate system (two opposite axial edges simply supported and arbitrary boundary conditions at the curved edges).

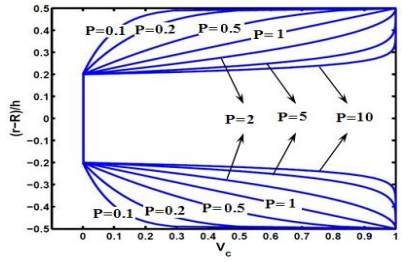

Fig.2
Variation of the fiber volume fraction (V_c) through the thickness of the FG graded sheets ($b=0$, $c=2$).

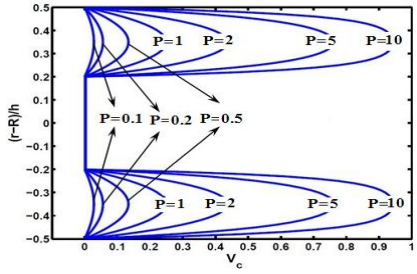

Fig.3
Variation of the fiber volume fraction (V_c) through the thickness of the FG graded sheets ($b=1$, $c=2$).

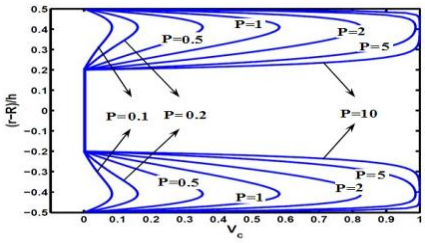

Fig.4
Variation of the fiber volume fraction (V_c) through the thickness of the FG graded sheets ($b=1$, $c=6$).

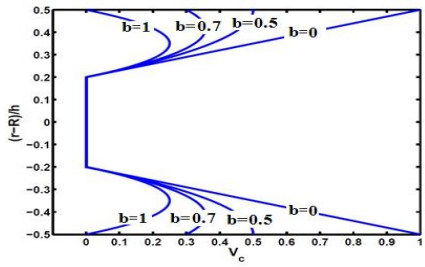

Fig.5
Variation of the fiber volume fraction (V_c) through the thickness of the FG graded sheets ($c=2$).

The relevant material properties for the constituent materials are as follows [15]
Metal (Aluminum, Al):

$$E_m = 70*109\ \text{Pa}, \rho_m = 2702\ \text{Kg/m3}, \upsilon_{\text{m}} = 0.3$$

Ceramic (Alumina, Al2O3):

$$E_c = 380*109\ \text{Pa}, \rho_c = 3800\ \text{Kg/m3}, \upsilon_{\text{c}} = 0.3$$

3 GOVERNING EQUATIONS

The mechanical constitutive relation that relates the stresses to the strains are as follows:

$$\begin{bmatrix} \sigma_r \\ \sigma_\theta \\ \sigma_z \\ \tau_{z\theta} \\ \tau_{rz} \\ \tau_{r\theta} \end{bmatrix} = \begin{bmatrix} C_{11} & C_{12} & C_{13} & 0 & 0 & 0 \\ C_{12} & C_{22} & C_{23} & 0 & 0 & 0 \\ C_{13} & C_{23} & C_{33} & 0 & 0 & 0 \\ 0 & 0 & 0 & C_{44} & 0 & 0 \\ 0 & 0 & 0 & 0 & C_{55} & 0 \\ 0 & 0 & 0 & 0 & 0 & C_{66} \end{bmatrix} \begin{bmatrix} \varepsilon_r \\ \varepsilon_\theta \\ \varepsilon_z \\ \gamma_{z\theta} \\ \gamma_{rz} \\ \gamma_{r\theta} \end{bmatrix} \tag{2}$$

In the absence of body forces, the governing equations are as follows:

$$\begin{aligned} &\frac{\partial \sigma_r}{\partial r} + \frac{1}{r}\frac{\partial \tau_{r\theta}}{\partial \theta} + \frac{\partial \tau_{rz}}{\partial z} + \frac{\sigma_r - \sigma_\theta}{r} = \rho \frac{\partial^2 u_r}{\partial t^2}, \\ &\frac{\partial \tau_{r\theta}}{\partial r} + \frac{1}{r}\frac{\partial \sigma_\theta}{\partial \theta} + \frac{\partial \tau_{\theta z}}{\partial z} + \frac{2\tau_{r\theta}}{r} = \rho \frac{\partial^2 u_\theta}{\partial t^2}, \\ &\frac{\partial \tau_{rz}}{\partial r} + \frac{1}{r}\frac{\partial \tau_{\theta z}}{\partial \theta} + \frac{\partial \sigma_z}{\partial z} + \frac{\tau_{rz}}{r} = \rho \frac{\partial^2 u_z}{\partial t^2} \end{aligned} \tag{3}$$

Strain-displacement relations are expressed as:

$$\varepsilon_r = \frac{\partial u_r}{\partial r}, \varepsilon_\theta = \frac{u_r}{r} + \frac{1}{r}\frac{\partial u_\theta}{\partial \theta}, \varepsilon_z = \frac{\partial u_z}{\partial z},$$
$$\gamma_{\theta z} = \frac{\partial u_\theta}{\partial z} + \frac{1}{r}\frac{\partial u_z}{\partial \theta}, \gamma_{rz} = \frac{\partial u_r}{\partial z} + \frac{\partial u_z}{\partial r}, \gamma_{r\theta} = \frac{1}{r}\frac{\partial u_r}{\partial \theta} + \frac{\partial u_\theta}{\partial r} - \frac{u_\theta}{r} \tag{4}$$

where u_r , u_ϑ and u_z are radial, circumferential and axial displacement components, respectively. Upon substitution Eq. (4) into (2) and then into (3), the equations of motion in terms of displacement components with infinitesimal deformations can be written as:

$$\begin{bmatrix} F_{1r} & F_{1\theta} & F_{1z} \\ F_{2r} & F_{2\theta} & F_{2z} \\ F_{3r} & F_{3\theta} & F_{3z} \end{bmatrix} \begin{Bmatrix} u_r \\ u_\theta \\ u_z \end{Bmatrix} = \begin{Bmatrix} \rho \dfrac{\partial^2 u_r}{\partial t^2} \\ \rho \dfrac{\partial^2 u_\theta}{\partial t^2} \\ \rho \dfrac{\partial^2 u_z}{\partial t^2} \end{Bmatrix} \tag{5}$$

where coefficients F_{ij} are given in Appendix A.

The boundary conditions at the concave and convex surfaces, $r=r_i$ and r_o , respectively, can be described as follows:

$$\sigma_r = \tau_{rz} = \tau_{r\theta} = 0 \tag{6}$$

In this investigation, three different types of classical boundary conditions at edges z=0 and L_z of the finite panel can be stated as follows:

Simply supported (S):

$$U_r = U_\theta = \sigma_z = 0 \tag{7}$$

Clamped (C):

$$U_r = U_\theta = U_z = 0 \tag{8}$$

Free (F):

$$\sigma_z = \tau_{z\theta} = \tau_{zr} = 0 \tag{9}$$

4 SOLUTION PROCEDURE

For the curved panels with simply supported at one pair of opposite edges, the displacement components can be expanded in terms of trigonometric functions in the direction normal to these edges. In this paper, it is assumed that the edges $\vartheta=0$ and $\vartheta=\Phi$ are simply supported. Hence,

$$u_r(r,\theta,z,t) = \sum_{m=1}^{\infty} U_r(r,z)\sin(\frac{m\pi}{\Phi}\theta)e^{i\omega t},$$
$$u_\theta(r,\theta,z,t) = \sum_{m=1}^{\infty} U_\theta(r,z)\cos(\frac{m\pi}{\Phi}\theta)e^{i\omega t}, \tag{10}$$
$$u_z(r,\theta,z,t) = \sum_{m=1}^{\infty} U_z(r,z)\sin(\frac{m\pi}{\Phi}\theta)e^{i\omega t}$$

where m is the circumferential wave number, ω is the natural frequency and i ($=\sqrt{-1}$) is the imaginary number. Substituting for displacement components from Eq. (10) into Eq. (5), and then using GDQ method to discretize the equations of motion (Eq. 5), one can get the following equations [A brief review of GDQ method is given in Appendix B]:

In the r direction:

$$\begin{aligned}
&(c_{11})_{ij}\sum_{n=1}^{N_r}B_{in}^{r}U_{rnj}+(c_{12})_{ij}\Big(\frac{m\pi}{\Phi r_i^2}U_{\theta ij}-\frac{m\pi}{\Phi r_i}\sum_{n=1}^{N_r}A_{in}^{r}U_{\theta nj}+\frac{1}{r_i}\sum_{n=1}^{N_r}A_{in}^{r}U_{rnj}-\\
&\frac{U_{rij}}{r_i^2}\Big)+(c_{13})_{ij}\sum_{n=1}^{N_r}\sum_{v=1}^{N_z}A_{jv}^{z}A_{in}^{r}U_{znv}+\Big(\frac{\partial c_{11}}{\partial r}\Big)_{ij}\sum_{n=1}^{N_r}A_{in}^{r}U_{rnj}+\Big(\frac{\partial c_{12}}{\partial r}\Big)_{ij}\Big(\frac{1}{r_i}U_{rij}-\\
&\frac{m\pi}{\Phi r_i}U_{\theta ij}\Big)+\Big(\frac{\partial c_{13}}{\partial r}\Big)_{ij}\sum_{n=1}^{N_z}A_{jn}^{z}U_{zin}+\frac{(c_{66})_{ij}}{r_i}\Big(-\frac{m\pi}{\Phi}\sum_{n=1}^{N_r}A_{in}^{r}U_{\theta nj}-\frac{1}{r_i}\Big(\frac{m\pi}{\Phi}\Big)^2U_{rij}\\
&+\frac{m\pi}{\Phi r_i}U_{\theta ij}\Big)+(c_{55})_{ij}\Big(\sum_{n=1}^{N_z}B_{jn}^{z}U_{rin}+\sum_{n=1}^{N_r}\sum_{v=1}^{N_z}A_{jv}^{z}A_{in}^{r}U_{znv}\Big)+\frac{1}{r_i}\Big((c_{11})_{ij}\sum_{n=1}^{N_r}A_{in}^{r}U_{rnj}\\
&+(c_{12})_{ij}\Big(\frac{U_{rij}}{r_i}-\frac{m\pi}{\Phi r_i}U_{\theta ij}\Big)+(c_{13})_{ij}\sum_{n=1}^{N_z}A_{jn}^{z}U_{zin}-(c_{12})_{ij}\sum_{n=1}^{N_r}A_{in}^{r}U_{rnj}-(c_{22})_{ij}\\
&\Big(\frac{U_{rij}}{r_i}-\frac{m\pi}{\Phi r_i}U_{\theta ij}\Big)-(c_{23})_{ij}\sum_{n=1}^{N_z}A_{jn}^{z}U_{zin}\Big)=-\rho_{ij}\omega^2U_{rij}
\end{aligned}\tag{11}$$

In the ϑ direction:

$$\begin{aligned}
&(c_{66})_{ij}\Big(-\frac{1}{r_i^2}\frac{m\pi}{\Phi}U_{rij}+\frac{m\pi}{\Phi r_i}\sum_{n=1}^{N_r}A_{in}^{r}U_{rnj}+\sum_{n=1}^{N_r}B_{in}^{r}U_{\theta nj}+\frac{U_{\theta ij}}{r_i^2}-\frac{1}{r_i}\sum_{n=1}^{N_r}A_{in}^{r}U_{\theta nj}\Big)\\
&+\Big(\frac{\partial c_{66}}{\partial r}\Big)_{ij}\Big(\frac{m\pi}{\Phi r_i}U_{rij}+\sum_{n=1}^{N_r}A_{in}^{r}U_{\theta nj}-\frac{U_{\theta ij}}{r_i}\Big)+\frac{1}{r_i}\Big((c_{12})_{ij}\frac{m\pi}{\Phi}\sum_{n=1}^{N_r}A_{in}^{r}U_{rnj}+(c_{22})_{ij}\\
&\Big(\frac{m\pi}{\Phi r_i}U_{rij}-\frac{1}{r_i}\Big(\frac{m\pi}{\Phi}\Big)^2U_{\theta ij}\Big)+(c_{23})_{ij}\frac{m\pi}{\Phi}\sum_{n=1}^{N_z}A_{jn}^{z}U_{zin}\Big)+(c_{44})_{ij}\Big(\sum_{n=1}^{N_z}B_{jn}^{z}U_{\theta in}+\\
&\frac{m\pi}{\Phi r_i}\sum_{n=1}^{N_z}A_{jn}^{z}U_{zin}\Big)+\frac{2(c_{66})_{ij}}{r_i}\Big(\frac{m\pi}{\Phi r_i}U_{rij}+\sum_{n=1}^{N_r}A_{in}^{r}U_{\theta nj}-\frac{U_{\theta ij}}{r_i}\Big)=-\rho_{ij}\omega^2U_{\theta ij}
\end{aligned}\tag{12}$$

In the z direction:

$$\begin{aligned}
&(c_{55})_{ij}\Big(\sum_{n=1}^{N_r}\sum_{v=1}^{N_z}A_{jv}^{z}A_{in}^{r}U_{rmv}+\sum_{n=1}^{N_r}B_{in}^{r}U_{znj}\Big)+\Big(\frac{\partial c_{55}}{\partial r}\Big)_{ij}\Big(\sum_{n=1}^{N_z}A_{jn}^{z}U_{rin}+\sum_{n=1}^{N_r}A_{in}^{r}U_{znj}\Big)\\
&+\frac{(c_{44})_{ij}}{r_i}\Big(-\frac{m\pi}{\Phi}\sum_{n=1}^{N_z}A_{jn}^{z}U_{\theta in}-\frac{1}{r_i}\Big(\frac{m\pi}{\Phi}\Big)^2U_{zij}\Big)+(c_{13})_{ij}\sum_{n=1}^{N_r}\sum_{v=1}^{N_z}A_{jv}^{z}A_{in}^{r}U_{rmv}+\\
&(c_{23})_{ij}\Big(\frac{1}{r_i}\sum_{n=1}^{N_z}A_{jn}^{z}U_{rin}-\frac{m\pi}{\Phi r_i}\sum_{n=1}^{N_z}A_{jn}^{z}U_{\theta in}\Big)+(c_{33})_{ij}\sum_{n=1}^{N_z}B_{jn}^{z}U_{zin}+\frac{(c_{55})_{ij}}{r_i}\\
&\Big(\sum_{n=1}^{N_z}A_{jn}^{z}U_{rin}+\sum_{n=1}^{N_r}A_{in}^{r}U_{znj}\Big)=-\rho_{ij}\omega^2U_{zij}
\end{aligned}\tag{13}$$

In the above-mentioned equations $i=2,\ldots,N_{r-1}$ and $j=2,\ldots,N_{z-1}$. A_{ij}^{r},A_{ij}^{z} and B_{ij}^{r},B_{ij}^{z} are the first and second order GDQ weighting coefficients in the r- and z-directions, respectively. Substituting for displacement components from

Eq. (10) into Eq. (6), and then using GDQ method to discretize the boundary conditions, one can get the following equations:

$$\begin{aligned}
&\sum_{n=1}^{N_z} A_{jn}^{z} U_{rin} + \sum_{n=1}^{N_r} A_{in}^{r} U_{znj} = 0, \\
&\frac{m\pi}{\Phi r_i} U_{rij} + \sum_{n=1}^{N_r} A_{in}^{r} U_{\theta nj} - \frac{U_{\theta ij}}{r_i} = 0, \\
&(c_{11})_{ij} \sum_{n=1}^{N_r} A_{in}^{r} U_{rnj} + (c_{12})_{ij} \left(\frac{U_{rij}}{r_i} - \frac{m\pi}{\Phi r_i} U_{\theta ij}\right) + (c_{13})_{ij} \sum_{n=1}^{N_z} A_{jn}^{z} U_{zin} = 0
\end{aligned} \tag{14}$$

where $i=1$ at $r=r_i$ and $i=N_r$ at $r=r_o$, and $j=1,2,\ldots,N_z$. By following the same procedure the boundary conditions at $z=0$ and L_z stated in Eqs. (7-9), become

Simply supported (S):

$$\begin{aligned}
&U_{rij} = U_{\theta ij} = 0, \\
&(c_{13})_{ij} \sum_{n=1}^{N_r} A_{in}^{r} U_{rnj} + (c_{23})_{ij} \left(\frac{U_{rij}}{r_i} - \frac{m\pi}{\Phi r_i} U_{\theta ij}\right) + (c_{33})_{ij} \sum_{n=1}^{N_z} A_{jn}^{z} U_{zin} = 0
\end{aligned} \tag{15}$$

Clamped (C):

$$U_{rij} = U_{\theta ij} = U_{zij}\, 0 \tag{16}$$

Free (F):

$$\begin{aligned}
&(c_{13})_{ij} \sum_{n=1}^{N_r} A_{in}^{r} U_{rnj} + (c_{23})_{ij} \left(\frac{U_{rij}}{r_i} - \frac{m\pi}{\Phi r_i} U_{\theta ij}\right) + (c_{33})_{ij} \sum_{n=1}^{N_z} A_{jn}^{z} U_{zin} = 0, \\
&\sum_{n=1}^{N_z} A_{jn}^{z} U_{\theta in} + \frac{m\pi}{\Phi r_i} U_{zij} = 0, \\
&\sum_{n=1}^{N_z} A_{jn}^{z} U_{rin} + \sum_{n=1}^{N_r} A_{in}^{r} U_{znj} = 0
\end{aligned} \tag{17}$$

In the above equations $i=2,\ldots,N_r-1$; also $j=1$ at $z=0$ and $j=N_z$ *at* $z=L_z$. In order to carry out the eigenvalue analysis, the domain and boundary nodal displacements should be separated. In vector forms, they are denoted as {d} and {b}, respectively. Based on this definition, the discretized form of the equations of motion and the related boundary conditions can be represented in the matrix form as:

Equations of motion, Eqs. (11-13):

$$\left[\left[K_{db}\right]\left[K_{dd}\right]\right]\begin{Bmatrix}\{b\}\\ \{d\}\end{Bmatrix} - \omega^2 \left[M\right]\{d\} = \{0\} \tag{18}$$

Boundary conditions, Eq. (14) and Eqs. (15-17):

$$\left[K_{bd}\right]\{d\} + \left[K_{bb}\right]\{b\} = \{0\} \tag{19}$$

Eliminating the boundary degrees of freedom in Eq. (18) using Eq. (19), this equation becomes,

$$\left[K\right] - \omega^2 \left[M\right]\{d\} = \{0\} \tag{20}$$

where $[K]=[K_{dd}]-[K_{db}][K_{bb}]^{-1}[K_{bd}]$. The above eigenvalue system of equations can be solved to find the natural frequencies and mode shapes of the curved panel.

5 NUMERICAL RESULTS AND DISCUSSION

To verify the proficiency of presented method and three-parameter model for volume fraction of FG materials, several numerical examples are carried out for comparisons. The results of the presented formulations are given in the form of convergence studies with respect to N_r and N_z, the number of discrete points distributed along the radial and axial directions, respectively. To validate the proposed approach its convergence and accuracy are demonstrated via different examples. The obtained natural frequencies based on the three-dimensional elasticity formulation are compared with those of the power series expansion method for FGM curved panels [12, 25, 26]. In these studies the material properties of functionally graded materials are assumed as follows:

Metal (Aluminum, Al):

$$E_m = 70*109 \text{ Pa}, \rho_m = 2702 \text{ Kg/m3}, \upsilon_m = 0.3$$

Ceramic (Alumina, Al2O3):

$$E_c = 380*109 \text{ Pa}, \rho_c = 3800 \text{ Kg/m3}, \upsilon_c = 0.3$$

Subscripts *M* and *C* refer to the metal and ceramic constituents which denote the material properties of the outer and inner surfaces of the panel, respectively. To validate the analysis, results for FGM cylindrical shells are compared with similar ones in the literature, as shown in Table 1. The comparison shows that the present results agreed well with those in the literatures. Besides fast rate of convergence of the method is quite evident, and it is found that only thirteen grid points (N_r= N_z=*13*) along the radial and axial directions can yield accurate results. Further validation of the present results for isotropic FGM cylindrical panel is shown in Table 2. In this Table, comparison is made for different L_z/R and L_z/h ratios, and as it is observed there is good agreement between the results. After demonstrating the convergence and accuracy of the present method, parametric studies for 3-D vibration analysis of thick FG sandwich curved panels with considering a three-parameter power-low distribution, length-to-mean radius ratio and different combinations of Free, Simply supported and Clamped boundary conditions at the curved edges, are computed. The boundary conditions of the panel are specified by the letter symbols, for example, *S-C-S-F* denotes a curved panel with edges $\vartheta=0$ and Φ simply supported (*S*), edge z=0 clamped (*C*), and edge z= L_z free (*F*). The non-dimensional natural frequency, Winkler and shearing layer elastic coefficients are as follows:

$$\Omega_{mn} = \omega_{mn} 10h\sqrt{\rho_c / E_c} \tag{21}$$

where ρ_c,E_c and G_c represent the mass density, Young's modulus and shear modulus of the ceramic, respectively.

The influence of the index *p* on the natural frequency is shown in Figs. 6 and 7. According to these figures the frequency parameter of laminated panels with ceramic layers rich is more than the natural frequency parameter of the limit cases of homogeneous layers of metal. It should be noticed that with the increase of ceramic volume fraction, the frequency parameter of the panels does not increase necessarily, so by considering suitable amounts of power-law index p $(0 \le p \le \infty)$ and the parameters *b* and *c*, one can get dynamic characteristics similar or better than the isotropic ceramic limit case for laminated FG curved panels. Fig. 6 shows that for p>3 and $(0 \le b < 1)$, The discrepancy between the natural frequencies of the panels, increase with the increase of *p* for different types of boundary conditions. For p<1 and $(0 \le b < 1)$, increasing of parameter *b* does not have significant effect on the amount of discrepancy between the natural frequencies of the panels. As can be seen from Fig. 7, with the increase of *p*, Firstly, the natural frequencies of the panels for different amounts of parameter *c* sharply increases and for the bigger amount of power-law index (p >3) decreases.

Table 1
Comparison of the normalized natural frequency of an FGM composite curved panel with four edges simply supported $(\Omega_{11}=\omega_{11}R\Phi\sqrt{\rho_m h/D}, D=E_m h^3/12(1-\upsilon_m^2))$.

P (volume fraction index)		R/L_z				
		0.5	1	5	10	50
0	Nr=Nz=5	69.9774	52.1052	42.7202	42.3717	42.2595
	Nr=Nz=7	69.9722	52.1052	42.7158	42.3718	42.2550
	Nr=Nz=9	69.9698	52.1003	42.7159	42.3700	42.2553
	Nr=Nz=11	69.9700	52.1003	42.7160	42.3677	42.2552
	Nr=Nz=13	69.9700	52.1003	42.7160	42.3677	42.2553
	Ref. [12]	68.8645	51.5216	42.2543	41.908	41.7963
0.2	Nr=Nz=5	65.1470	47.9393	39.1282	38.8010	38.7020
	Nr=Nz=7	65.4449	48.0456	39.1008	38.7366	38.6834
	Nr=Nz=9	65.4526	48.1340	39.0836	38.7568	38.6581
	Nr=Nz=11	65.4304	48.1340	39.0835	38.7568	38.6580
	Nr=Nz=13	65.4304	48.1340	39.0835	38.7568	38.6581
	Ref. [12]	64.4001	47.5968	40.1621	39.8472	39.7465
0.5	Nr=Nz=5	60.1196	43.5539	36.1264	35.8202	34.7341
	Nr=Nz=7	60.2769	43.7128	36.1401	35.7964	35.0677
	Nr=Nz=9	60.3574	43.7689	36.0944	35.7890	35.7032
	Nr=Nz=11	60.3574	43.7688	36.0943	35.7891	35.7032
	Nr=Nz=13	60.3574	43.7689	36.0944	35.7891	35.7032
	Ref. [12]	59.4396	43.3019	37.287	36.9995	36.9088
1	Nr=Nz=5	54.1034	38.5180	31.9860	30.7065	30.6336
	Nr=Nz=7	54.6039	39.1477	32.1140	31.6982	31.5397
	Nr=Nz=9	54.7141	39.1620	32.0401	31.7608	31.6877
	Nr=Nz=11	54.7141	39.1621	32.0401	31.7608	31.6878
	Nr=Nz=13	54.7141	39.1621	32.0401	31.7608	31.6877
	Ref. [12]	53.9296	38.7715	33.2268	32.9585	32.875
2	Nr=Nz=5	46.9016	34.7702	27.6657	27.4295	27.3725
	Nr=Nz=7	47.9865	34.6980	27.5733	27.3389	27.2669
	Nr=Nz=9	48.5250	34.6852	27.5614	27.3238	27.2663
	Nr=Nz=11	48.5250	34.6851	27.5614	27.3239	27.2663
	Nr=Nz=13	48.5250	34.6851	27.5614	27.3239	27.2662
	Ref. [12]	47.8259	34.3338	27.4449	27.1789	27.0961

Table 2
Comparison of the normalized natural frequency of an FGM composite curved panel for various L_Z/R and L_Z/h ratios.

			P (volume fraction index)				
			0	0.5	1	4	10
L_Z/h=2		L_Z/R=0.5					
	Ref. [26]		0.9334	0.8213	0.7483	0.6011	0.5461
	Ref. [25]		0.9187	0.8013	0.7263	0.5267	0.5245
	$N_r=N_z=5$		0.9342	0.8001	0.7149	0.5878	0.5133
	$N_r=N_z=7$		0.9249	0.8011	0.7250	0.5783	0.5298
	$N_r=N_z=9$		0.9250	0.8018	0.7253	0.5790	0.5301
	$N_r=N_z=11$		0.9249	0.8017	0.7253	0.5789	0.5300
	$N_r=N_z=13$		0.9250	0.8018	0.7252	0.5790	0.5301
	Ref. [26]	L_Z/R=1	0.9163	0.8105	0.7411	0.5967	0.5392
	Ref. [25]		0.8675	0.7578	0.6875	0.5475	0.4941
	$N_r=N_z=5$		0.8942	0.7531	0.6746	0.5741	0.4913
	$N_r=N_z=7$		0.8851	0.7671	0.6912	0.5599	0.5074
	$N_r=N_z=9$		0.8857	0.7666	0.6935	0.5531	0.5065
	$N_r=N_z=11$		0.8857	0.7667	0.6934	0.5531	0.5063
	$N_r=N_z=13$		0.8856	0.7667	0.6935	0.5532	0.5064
L_Z/h=5		L_Z/R=0.5					
	Ref. [26]		0.2153	0.1855	0.1678	0.1413	0.1328
	Ref. [25]		0.2113	0.1814	0.1639	0.1367	0.1271
	$N_r=N_z=5$		0.2230	0.1997	0.1542	0.1374	0.1373
	$N_r=N_z=7$		0.2176	0.1823	0.1624	0.1362	0.1233
	$N_r=N_z=9$		0.2130	0.1817	0.1639	0.1374	0.1296

$N_r=N_z=11$		0.2128	0.1816	0.1640	0.1377	0.1296
$N_r=N_z=13$		0.2129	0.1817	0.1640	0.1374	0.1295
Ref. [26]	$L_z/R=1$	0.2239	0.1945	0.1769	0.1483	0.1385
Ref. [25]		0.2164	0.1879	0.1676	0.1394	0.1286
$N_r=N_z=5$		0.2066	0.1765	0.1567	0.1476	0.1409
$N_r=N_z=7$		0.2133	0.1843	0.1688	0.1377	0.1288
$N_r=N_z=9$		0.2154	0.1848	0.1671	0.1392	0.1301
$N_r=N_z=11$		0.2155	0.1847	0.1675	0.1392	0.1299
$N_r=N_z=13$		0.2155	0.1847	0.1671	0.1392	0.1302

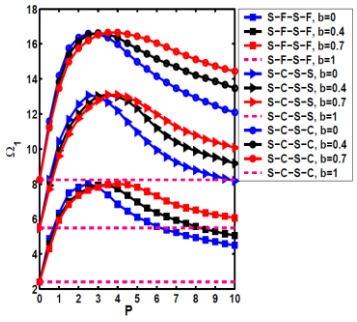

Fig.6
The first non-dimensional natural frequency of FG laminated curved panels versus p for different amounts of b and types of boundary conditions including *S-C-S-C, S-C-S-S, S-F-S-F* ($c=1$, $R/h=L_z/R=10$, $\Phi=180°$)**.**

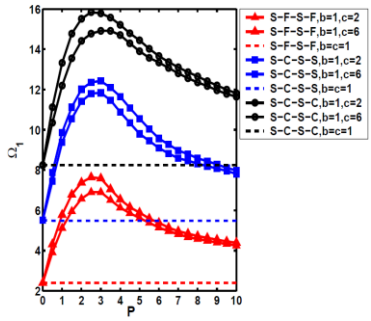

Fig.7
The first non-dimensional natural frequency of FG laminated curved panels versus p for different amounts of c and types of boundary conditions including *S-C-S-C, S-C-S-S, S-F-S-F* ($R/h=L_z/R=10$, $\Phi=180°$).

In Fig. 8 the effects of variation of circumferential wave numbers (m) on the frequency parameters of *S-C-S-C* sandwich curved panel for different values of L_z/R ratio are demonstrated. According to Fig. 8, the general behavior of the frequency parameters of sandwich panels for all L_z/R ratios is that the frequency parameters converge only in the range beyond that of the fundamental frequency parameters. This means that the effects of the L_z/R ratios are more prominent at low circumferential wave numbers, particularly those in the range before that of the fundamental frequency parameters, than at high circumferential wave numbers. It is also seen from Fig. 8 that the frequency parameter decreases rapidly with the increase of the length-to-mean radius ratio (L_z/R) and then remains almost unaltered for the long cylindrical panel.

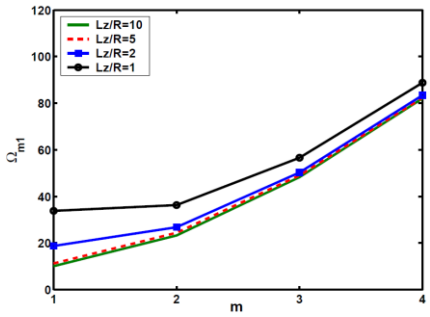

Fig.8
Variation of circumferential wave numbers (m) with the frequency parameters of *S-C-S-C* FG laminated curved panels ($p=1$, $c=1$, $b=0.4$, $R/h=10$, $\Phi=180°$).

6 CONCLUSIONS

In this research, free vibration of a thick finite FG layers panel is investigated based on three-dimensional theory of elasticity. Three complicated equations of motion for the curved panel under consideration are semi-analytically solved by two-dimensional generalized differential quadrature method (2-D GDQM). Using the 2-D GDQ method along the radial and axial directions, allows one to deal with curved panel with arbitrary thickness distribution of material properties in an exact manner. The material properties vary continuously through the layers thickness according to a three-parameter power-low distribution. It is assumed that the inner surfaces of the FG sheets are metal rich while the outer surfaces of the layers can be metal rich, ceramic rich or made of a mixture of two constituents. The effects of different geometrical parameters, different profiles of fiber volume fraction and three parameters of power-law distribution on the vibration characteristics of the laminated curved panels are investigated. From this study, some conclusions can be made:

- Results show that the frequency parameter of laminated panels with ceramic layers rich is more than the natural frequency parameter of the limit cases of homogeneous layers of metal. It should be noticed that with the increase of ceramic volume fraction, the frequency parameter of the panels does not increase necessarily, so by considering suitable amounts of power-law index p $(0 \le p \le \infty)$ and the parameters b and c, one can get dynamic characteristics similar or better than the isotropic ceramic limit case for laminated FG curved panels.
- It is observed that for p>3 and $(0 \le b < 1)$, The discrepancy between the natural frequencies of the panels, increase with the increase of p for different types of boundary conditions. For p<1 and $(0 \le b < 1)$, increasing of parameter b does not have significant effect on the amount of discrepancy between the natural frequencies of the panels.
- It is observed that with the increase of p, the discrepancy between the natural frequencies of the panels for different amounts of parameter c sharply decreases.
- It can be found that the general behavior of the frequency parameters of sandwich panels for all L_z/R ratios is that the frequency parameters converge only in the range beyond that of the fundamental frequency parameters. This means that the effects of the L_z/R ratios are more prominent at low circumferential wave numbers, particularly those in the range before that of the fundamental frequency parameters, than at high circumferential wave numbers.
- The frequency parameter decreases rapidly with the increase of the length-to-mean radius ratio (L_z/R) and then remains almost unaltered for the long cylindrical panels.

APPENDIX A

$$F_{1r} = c_{11}\frac{\partial^2}{\partial r^2} + \frac{\partial c_{11}}{\partial r}\frac{\partial}{\partial r} + \frac{\partial c_{12}}{r\partial r} + \frac{c_{66}}{r^2}\frac{\partial^2}{\partial \theta^2} + c_{55}\frac{\partial^2}{\partial z^2} + \frac{c_{11}}{r}\frac{\partial}{\partial r} - \frac{c_{22}}{r^2}$$

$$F_{1\theta} = -\frac{c_{12}}{r^2}\frac{\partial}{\partial \theta} + \frac{c_{12}}{r}\frac{\partial^2}{\partial r\partial \theta} + \frac{\partial c_{12}}{r\partial r}\frac{\partial}{\partial \theta} + \frac{c_{66}}{r}\frac{\partial^2}{\partial \theta \partial r} - \frac{c_{66}}{r^2}\frac{\partial}{\partial \theta} + \frac{c_{12}}{r^2}\frac{\partial}{\partial \theta} - \frac{c_{22}}{r^2}\frac{\partial}{\partial \theta}$$

$$F_{1z} = c_{13}\frac{\partial^2}{\partial r\partial z} + \frac{\partial c_{13}}{\partial r}\frac{\partial}{\partial z} + c_{55}\frac{\partial^2}{\partial z\partial r} + \frac{c_{13}}{r}\frac{\partial}{\partial z} - \frac{c_{23}}{r}\frac{\partial}{\partial z}$$

$$F_{2r} = \frac{c_{66}}{r}\frac{\partial^2}{\partial r\partial \theta} + \frac{\partial c_{66}}{r\partial r}\frac{\partial}{\partial \theta} + \frac{c_{12}}{r}\frac{\partial^2}{\partial r\partial \theta} + \frac{c_{22}}{r^2}\frac{\partial}{\partial \theta} + \frac{c_{66}}{r^2}\frac{\partial}{\partial \theta}$$

$$F_{2\theta} = c_{66}\frac{\partial^2}{\partial r^2} + \frac{\partial c_{66}}{\partial r}\frac{\partial}{\partial r} - \frac{\partial c_{66}}{r\partial r} + \frac{c_{22}}{r^2}\frac{\partial^2}{\partial \theta^2} + c_{44}\frac{\partial^2}{\partial z^2} + \frac{c_{66}}{r}\frac{\partial}{\partial r} - \frac{c_{66}}{r^2}$$

$$F_{2z} = \frac{c_{23}}{r}\frac{\partial^2}{\partial \theta \partial z} + \frac{c_{44}}{r}\frac{\partial^2}{\partial z\partial \theta} \qquad F_{3r} = c_{55}\frac{\partial^2}{\partial r\partial z} + \frac{\partial c_{55}}{\partial r}\frac{\partial}{\partial z} + c_{13}\frac{\partial^2}{\partial z\partial r} + \frac{c_{23}}{r}\frac{\partial}{\partial z} + \frac{c_{55}}{r}\frac{\partial}{\partial z}$$

$$F_{3\theta} = \frac{c_{44}}{r}\frac{\partial^2}{\partial \theta \partial z} + \frac{c_{23}}{r}\frac{\partial^2}{\partial \theta \partial z} \qquad F_{3z} = c_{55}\frac{\partial^2}{\partial r^2} + \frac{\partial c_{55}}{\partial r}\frac{\partial}{\partial r} + \frac{c_{44}}{r^2}\frac{\partial^2}{\partial \theta^2} + c_{33}\frac{\partial^2}{\partial z^2} + \frac{c_{55}}{r}\frac{\partial}{\partial r}$$

APPENDIX B

In GDQ method, the *n*th order partial derivative of a continuous function $f(x,z)$ with respect to *x* at a given point *xi* can be approximated as a linear summation of weighted function values at all the discrete points in the domain of *x*, that is

$$\frac{\partial^n f(x_i,z)}{\partial x^n}=\sum_{k=1}^{N} c_{ik}^{n} f(x_{ik},z) \quad (i=1,2,...,N, n=1,2,...,N-1) \tag{B.1}$$

where *N* is the number of sampling points and c_{ij}^{n} is the *xi* dependent weight coefficient. To determine the weighting coefficients c_{ij}^{n}, the Lagrange interpolation basic functions are used as the test functions, and explicit formulas for computing these weighting coefficients can be obtained as [34, 35]

$$c_{ij}^{(1)}=\frac{M^{(1)}(x_i)}{(x_i-x_j)M^{(1)}(x_j)}, \quad i,j=1,2,...,N, \quad i\neq j \tag{B.2}$$

where

$$M^{(1)}(x_i)=\prod_{j=1,i\neq j}^{N}(x_i-x_j) \tag{B.3}$$

and for higher order derivatives, one can use the following relations iteratively

$$c_{ij}^{(n)}=n(c_{ii}^{(n-1)}c_{ij}^{1}-\frac{c_{ij}^{(n-1)}}{(x_i-x_j)}), \quad i,j=1,2,...,N, \quad i\neq j, \quad n=2,3,...,N-1 \tag{B.4}$$

$$c_{ii}^{(n)}=-\sum_{j=1,i\neq j}^{N} c_{ij}^{(n)} \quad i=1,2,...,N, \quad n=1,2,...,N-1 \tag{B.5}$$

A simple and natural choice of the grid distribution is the uniform grid-spacing rule. However, it was found that nonuniform grid-spacing yields result with better accuracy. Hence, in this work, the Chebyshev-Gauss-Lobatto quadrature points are used [35]

$$x_i=\frac{1}{2}(1-\cos(\frac{i-1}{N-1}\pi)) \quad i=1,2,...,N \tag{B.6}$$

REFERENCES

[1] Abrate S., 1998, *Impact on Composite Structures*, Cambridge UK, Cambridge University Press.
[2] Viola E., Tornabene F., 2009, Free vibrations of three-parameter functionally graded parabolic panels of revolution, *Mechanics Research Communications* **36**: 587-594.
[3] Anderson T.A., 2003, 3D elasticity solution for a sandwich composite with functionally graded core subjected to transverse loading by a rigid sphere, *Composite Structure* **60**: 265-274.
[4] Kashtalyan M., Menshykova M., 2009, Three-dimensional elasticity solution for sandwich panels with a functionally graded core, *Composite Structure* **87**: 36-43.

[5] Li Q., Iu V.P., Kou K.P., 2008, Three-dimensional vibration analysis of functionally graded material sandwich plates, *Journal of Sound and Vibration* **311**(1-2): 498-515.

[6] Zenkour A.M., 2005, A comprehensive analysis of functionally graded sandwich plates. Part 1-deflection and stresses, *International Journal of Solid Structure* **42**: 5224-5242.

[7] Zenkour A.M., 2005, A comprehensive analysis of functionally graded sandwich plates : Part 1- Deflection and stresses, *International Journal of Solid Structure* **42**: 5243-5258.

[8] Kamarian S., Yas M.H., Pourasghar A., 2013, Free vibration analysis of three-parameter functionally graded material sandwich plates resting on Pasternak foundations, *Sandwich Structure and Material* **15**: 292-308.

[9] Loy C.T., Lam K.Y., Reddy J.N., 1999, Vibration of functionally graded cylindrical shells, *International Journal of Mechanical science* **41**: 309-324.

[10] Pradhan S.C., Loy C.T., Lam K.Y., Reddy J.N., 2000, Vibration characteristic of functionally graded cylindrical shells under various boundary conditions, *Applied Acoustic* **61**: 119-129.

[11] Patel B.P., Gupta S.S., Loknath M.S.B., Kadu C.P., 2005, Free vibration analysis of functionally graded elliptical cylindrical shells using higher-order theory, *Composite Structure* **69**: 259-270.

[12] Pradyumna S., Bandyopadhyay J.N., 2008, Free vibration analysis of functionally graded panels using higher-order finite-element formulation, *Journal of Sound and Vibration* **318**: 176-192.

[13] Yang J., Shen S.H., 2003, Free vibration and parametric resonance of shear deformable functionally graded cylindrical panels, *Journal of Sound and Vibration* **261**: 871-893.

[14] Gang S.W., Lam K.Y., Reddy J.N., 1999, The elastic response of functionally graded cylindrical shells to low-velocity, *International Journal of Impact Engineering* **22**: 397-417.

[15] Shakeri M., Akhlaghi M., Hosseini S.M., 2006, Vibration and radial wave propagation velocity in functionally graded thick hollow cylinder, *Composite Structure* **76**: 174-181.

[16] Chen W.Q., Bian Z.G., Ding H.U., 2004, Three-dimensional vibration analysis of fluid-filled orthotropic FGM cylindrical shells, *International Journal of Mechanical Scienc*e **46**: 159-171.

[17] Tornabene F., 2009, Free vibration analysis of functionally graded conical cylindrical shell and annular plate structures with a four-parameter power-law distribution, *Computer Methods Applied Mechanical Engineering* **198**: 2911-2935.

[18] Sobhani Aragh B., Yas M.H., 2010, Static and free vibration analyses of continuously graded fiber-reinforced cylindrical shells using generalized power-law distribution, *Acta Mechanica* **215**: 155-173.

[19] Sobhani Aragh B., Yas M.H., 2010, Three dimensional free vibration of functionally graded fiber orientation and volume fraction of cylindrical panels, *Material Design* **31**: 4543-4552.

[20] Paliwal D.N., Kanagasabapathy H., Gupta K.M., 1995, The large deflection of an orthotropic cylindrical shell on a Pasternak foundation, *Composite Structure* **31**: 31-37.

[21] Paliwal D.N., Pandey R.K., Nath T., 1996, Free vibration of circular cylindrical shell on Winkler and Pasternak foundation, *International Journal of Pressure Vessels and Piping* **69**: 79-89.

[22] Yang R., Kameda H., Takada S., 1998, Shell model FEM analysis of buried pipelines under seismic loading, *Bulletin of the Disaster Prevention Research Institute* **38**: 115-146.

[23] Cai J.B., Chen W.Q., Ye G.R, Ding H.J., 2000, On natural frequencies of a transversely isotropic cylindrical panel on a kerr foundation, *Journal of Sound and Vibration* **232**: 997-1004.

[24] Gunawan H., TjMikami T., Kanie S., Sato M., 2006, Free vibration characteristics of cylindrical shells partially buried in elastic foundations, *Journal of Sound and Vibration* **290**: 785-793.

[25] Farid M., Zahedinejad P., Malekzadeh P., 2010, Three dimensional temperature dependent free vibration analysis of functionally graded material curved panels resting on two parameter elastic foundation using a hybrid semi-analytic, differential quadrature method, *Material Design* **31**: 2-13.

[26] Matsunaga H., 2008, Free vibration and stability of functionally graded shallow shells according to a 2-D higher-order deformation theory, *Composite Structure* **84**: 132-146.

[27] Civalek Ö., 2005, Geometrically nonlinear dynamic analysis of doubly curved isotropic shells resting on elastic foundation by a combination of HDQ-FD methods, *International Journal of Pressure Vessels and Piping* **82**: 470-479.

[28] Yas M.H., Tahouneh V., 2012, 3-D free vibration analysis of thick functionally graded annular plates on Pasternak elastic foundation via differential quadrature method (DQM), *Acta Mechanica* **223**: 43-62.

[29] Tahouneh V., Yas M.H., 2012, 3-D free vibration analysis of thick functionally graded annular sector plates on Pasternak elastic foundation via 2-D differential quadrature method, *Acta Mechanica* **223**: 1879-1897.

[30] Tahouneh V., Yas M.H., Tourang H., Kabirian M., 2013, Semi-analytical solution for three-dimensional vibration of thick continuous grading fiber reinforced (CGFR) annular plates on Pasternak elastic foundations with arbitrary boundary conditions on their circular edges, *Meccanica* **48**: 1313-1336.

[31] Tahouneh V., Yas M.H., 2013, Influence of equivalent continuum model based on the eshelby-mori-tanaka scheme on the vibrational response of elastically supported thick continuously graded carbon nanotube-reinforced annular plates, *Polymer Composites* **35**(8):1644-1661.

[32] Tahouneh V., Naei M.H., 2013, A novel 2-D six-parameter power-law distribution for three-dimensional dynamic analysis of thick multi-directional functionally graded rectangular plates resting on a two-parameter elastic foundation, *Meccanica* **49**(1):91-109.

[33] Tahouneh V., 2014, Free vibration analysis of thick CGFR annular sector plates resting on elastic foundations, *Structural Engineering and Mechanics* **50** (6): 773-796.

[34] Shu C., 2000, *Differential Quadrature and Its Application in Engineering*, Springer, Berlin.
[35] Shu C., Richards B.E., 1992, Application of generalized differential quadrature to solve two-dimensional incompressible Navier-Stokes equations , *International Journal for Numerical Methods in Fluids* **15**: 791-798.